Numerical evaluation of grouting scenarios for reducing water inflows in underground excavations – Goldcorp's Éléonore mine study case

Domingue C[1], Lemieux JM[1], Grenon M[2], Therrien R[1], Molson J[1], Lajoie PL[3] & Blessent D[4]

[1]*Faculté des sciences et de génie, Département de génie géologique et géologie, Université Laval, Québec, Canada*

[2]*Faculté des sciences et de génie, Département de génie des mines, de la métallurgie et des matériaux, Université Laval, Québec, Canada*

[3]*Goldcorp – Eleonore mine, Québec, Canada*

[4]*Department of Environmental Engineering, University of Medelin, Medelin, Antioquia, Coloombia*

ABSTRACT

Water inflows through fracture networks are one of the many challenges that the Éléonore mine has to face. Although pre-grouting of pilot holes during mine development has been proven to efficiently reduce water inflows into mine excavations, the actual design methods are empirical and can be optimized to increase grouting efficiency and decrease the associated costs. Optimization of the amount of cement needed for pre-grouting is achieved by designing the grouting approach based on the location of major faults around the excavations. Here, a base case finite-element numerical model and associated sensitivity analyses are used to simulate groundwater inflows into a stope, based on the Éléonore mining site characteristics. Simulations are conducted for testing various grout injection scenarios for various major fault locations around the stope. Sensitivity analyses have shown that for a fault located above the stope, the inflow reduction is greater when the zone between the fault and the stope is grouted instead of directly grouting the fault itself. Also, in the case of a fault intersecting a stope, the results have demonstrated that the fault itself should be grouted as widely as possible, instead of sealing only the immediate surroundings of the stope.

CITATION

Domingue C, Lemieux JM, Grenon M, Therrien R, Molson J, Jaloie PL & Blessent D. Numerical evaluation of grouting scenarios for reducing water inflows in underground excavations – Goldcorp's Éléonore mine study case. Proceedings of GeoOttawa 2017: Paper #335, Ottawa, Ontario, Canada. (2017) 7p.

This is the author's version of the original manuscript.
The final publication is available in the Proceedings of GeoOttawa 2017

1 INTRODUCTION

Groundwater infiltration into underground excavations represents a major engineering challenge, whether occurring in tunnels, potential geological repositories for nuclear wastes or in underground mines. In most of these cases, fractures and faults have been identified as the source of water infiltration. As stated by Coli & Pinzani (2014), the properties of discontinuities such as orientation, persistence, aperture, spacing, frequency and roughness have considerable impact on the permeability of the host rock. To mitigate this water infiltration through fracture networks or major faults, pre-grouting with pilot holes has been widely used and has been proven to efficiently reduce inflows in potential nuclear repository sites (Hernqvist & al., 2009) and tunneling (Holmøy & Nilsen, 2014). Pre-grouting consists of drilling pilot holes, in a specific repeated pattern to seal the water-transmissive discontinuities. When a discontinuity is encountered, a cement mix is injected through the drilled holes at the required pressure to reach and seal the conductive features. A conceptual design of pre-grouting is shown in Figure 1.

The Éléonore mine, located near James Bay Canada, faces groundwater infiltration due to discontinuities which provide a preferential flow path for groundwater. Pumping and pre-grouting have proven to efficiently reduce and control infiltration at the mining site. Pre-grouting, for example, is used almost systematically by applying fans of variously oriented pilot holes. Even if the water inflows have been reduced, the approach could be improved in a way to reduce the quantities and costs associated with cement injection through systematic pilot holes. Optimization of the method with designs based on the projected location of major water-bearing discontinuities is investigated here, through 2D numerical modelling of groundwater flow.

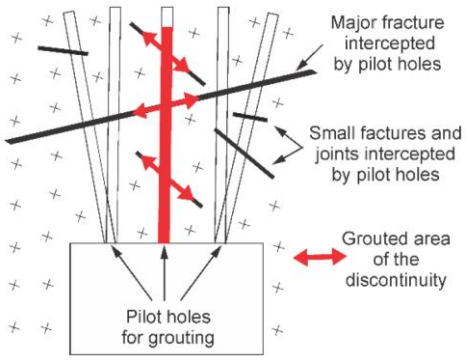

Figure 1. Section view of an overcut drift with the pre-grouting approach (adapted from Hernqvist & *al.*, 2009)

2 ELEONORE MINE SITE

The Éléonore mine is located in the James Bay area, on the shore of the Opinaca hydroelectric reservoir, about 800 km north of Montreal (Figure 2).

Éléonore is a gold-bearing underground mine, with a sub-vertical orebody. Longitudinal and transverse long-hole mining methods are used to mine the orebody. Two shafts and one ramp provide access to the mine. The shafts, for exploration and production, reach depths of 725 m and 1180 m, respectively. Hauling drift cross-section dimensions extend up to 5.5 × 5.5 meters and typical dimensions of the stopes are 35 × 30 × 8 meters.

Figure 2. Éléonore mine site location (Goldcorp Inc., 2017)

2.1 Geological settings

At the regional scale, the Éléonore mine is located at the junction of the sub-provinces Opinaca and LaGrande, respectively, which are composed of metasedimentary and volcano-plutonic rocks, intersected by diabase dykes.

At the local scale, the Éléonore mine is centered on a tonalite-diorite intrusion, the Lake Ell intrusion (Ravenelle & *al.*, 2010). The gold mineralization is mainly constricted in metasomatized wacke and appears as sub-parallel and sub-vertical lenses in a greywacke matrix (Ravenelle & *al.*, 2010). The lenses extend up to 1500 meters deep and their occurrence is apparently strongly linked to the structural regime (Fontaine & *al.,* 2015).

2.2 Structural context

The structural regime is dominated by four major fracture sets, counting one sub-horizontal set and three sub-verticals sets. In addition to these fracture sets, 21 major geological structures have been identified (Goldcorp Inc., 2014). From these structures, which are mostly sub-horizontal and sub-vertical, six are highly permeable. These permeable structures are considered as faults for the purpose of this paper. Also, secondary discontinuities have been observed in the surroundings of these faults, with an increasing permeability when located closer to the fault. Buffer zones of respectively 10 m and 20 m between the faults and the walls or the roof were recommended when designing the underground openings.

2.3 Hydrogeological setting

The mine is located under the Opinaca hydroelectric reservoir, which covers an area of 1000 km². The water level of the reservoir is controlled by Hydro-Quebec and the variation is inter-annual, between 211 and 217 m, depending on the company needs (Golder Associates Ltd, 2009). Measured hydraulic heads in the mine surroundings were comparable to the topographic elevation (Golder Associates Ltd, 2009).

The permeability of the lithological units was established by pumping tests and packer tests, before mine construction (Golder Associates Ltd, 2009). A numerical model simulating groundwater flow was developed, for which the rock mass was divided into five hydrogeological areas of variable hydraulic conductivity (K), decreasing with depth, from 1.0×10^{-5} m/s to 1.0×10^{-8} m/s. One exception to this tendency was observed between depths of 300 m and 360 m, where K is about two orders of magnitude higher than the hydraulic conductivity of the hydrogeological unit above (Golder Associates Ltd, 2009). The rock mass was considered as an equivalent porous medium for this study. The fractures and faults were neglected due to the poor definition of the structural regime at the time.

In order to improve the understanding of groundwater flow dynamics at the mine scale, another hydrogeological 3D control volume finite-element model was built, in which the porous medium was coupled to the major structures which were represented as discrete features. This model showed that the hydraulic conductivity was possibly two

orders of magnitude lower than previously stated when the major structures were considered as discrete features. The 3D modelling results suggested that the hydraulic conductivity of the hydrostratigraphic units could vary between $1.0x10^{-8}$ m/s and $1.0×10^{-10}$ m/s. Also, it was found that the aperture of the major structures could vary between $7.5×10^{-4}$ m and $1.0×10^{-6}$ m (Domingue, 2017).

Since the operations started, a database has been established to gather and facilitate access to all reported water inflows, their magnitude, location and grouting details. The encountered water inflows can reach up to 250 USgpm in some areas. Such water inflows need to be controlled and mitigation protocols have been set in place.

2.4 Mitigation methods

Mitigation methods for groundwater infiltration at the Éléonore mine are pumping and pre-grouting. Pre-grouting is the most common and efficient approach to control newly encountered infiltrations when drilling. Usually, pilot holes are drilled in a fan design into the stope face. When high pressures are encountered, drilling stops and a first injection of Portland cement is performed. Drilling is resumed and if water outflows are still detected at the same depth, grouting is repeated with an increased injection pressure. Once the pump capacity is reached, the operation stops and another grouting mix with an increased ratio of cement/water is then injected. Experience at the site has shown that the influence radius of pre-grouting from a test hole is about 1.5 m.

Pre-grouting has been observed as an efficient way to mitigate the water infiltration. However, the systematic approach could be optimized by quantifying its efficiency and adapting it depending on the location of major water-bearing faults.

3 METHODS AND MODELS

To evaluate the pre-grouting efficiency, two 2D onceptual models of a stope with a conductive fault nearby have been built (Figure 3). Model A is created with a fault above the stope and Model B is set with a fault intersecting the stope.

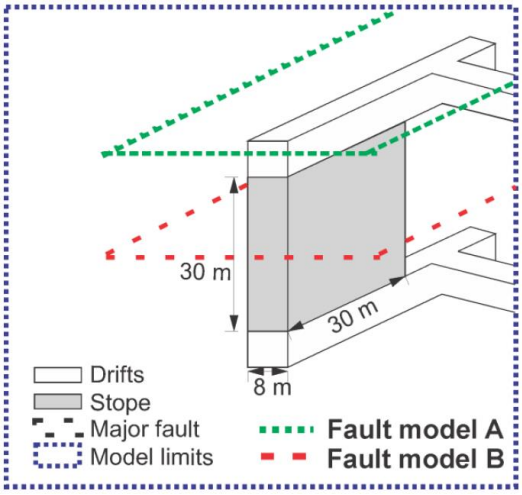

Figure 3. Conceptual Models A and B

For each conceptual model, a 2D hydrogeological model was built with the FLONET/TR2 code (Molson & Frind, 2017), which is a finite element code for 2D groundwater flow in saturated media. The code simulates hydraulic heads and velocities, which are the required data for this study.

For both conceptual models, a sensitivity analysis on several grouting scenarios is conducted to quantify the reduction of inflow into the stope.

3.1 Numerical model

The FLONET/TR2 code combines the hydraulic potential and streamfunction flow equations (Molson & Frind, 2017). The assumptions include constant temperature, a saturated and non-deforming medium, and steady-state conditions.

For both hydrogeological models, the model domain is an area of 100 m × 100 m, with a centered stope of 30 m × 8 m. For Model A, a 1 meter thick fault represented as an equivalent porous medium, is located 2 meters above the stope and extends to the model boundaries. For Model B, the fault is centered in the stope and also extends to the model boundaries.

The mesh is made of 200 element columns of 0.5 m in the x-direction and 115 element rows of 1 m or 0.25 m in the y-direction. The element height in the y-direction is generally 1 m, except for a refined area of 5 m near the fault. The elements of this specific refined zone are consequently 0.25 m high.

3.2 Boundary conditions

Boundary conditions are the same for Models A and B. Each lateral boundary of the models is set with a Neumann no-flow condition and each node of the stope boundaries is fixed with an internal Dirichlet prescribed hydraulic head value of 0 m (Figure 4).

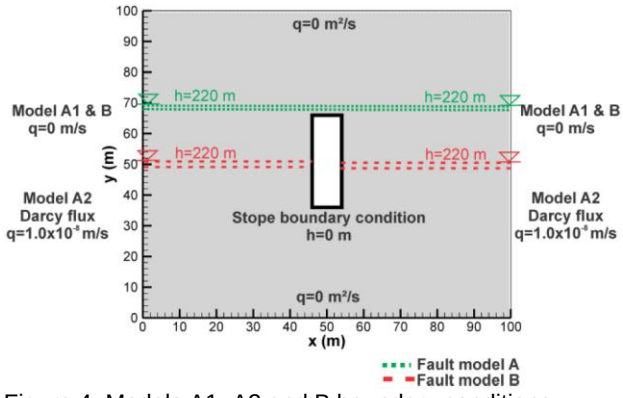

Figure 4. Models A1, A2 and B boundary conditions

For the fault, a Dirichlet condition of fixed hydraulic head is set at both of its intersections with the model boundaries. A fixed head of 220 m is set, corresponding to an average value of the topographic elevation, which is assumed as the hydraulic head for the domain under hydrostatic conditions.

A regional gradient was generated in Model A by imposing a Darcy flux along the left and right boundaries of 1.0×10^{-8} m/s (Figure 4). From this point, there's a distinction between Model A1, without regional flow, and Model A2, with regional flow.

3.3 Margins Hydraulic properties

The model material properties are based upon the 3D hydrogeological porous media model coupled to discrete features mentioned in Section 2.3 (Domingue, 2017). The host rock hydraulic conductivity is assumed homogeneous and is fixed at 1.0×10-8 m/s, in accordance with the 3D modelling results near level 230. The hydraulic conductivity of the cement is variable and represents the primary variable parameter for the sensitivity analysis.

The fault itself has an apparent hydraulic conductivity calculated from the hydraulic aperture of the fault. In order to create a worst case scenario, the maximum hydraulic aperture (2b) of a fault was considered, which corresponds to 7.5×10-4 m. The apparent hydraulic conductivity (Ka) of the fault is then computed from:

$$K_a = \frac{\rho\, g\, (2b)^3}{(\Delta z) 12 \mu} \qquad [1]$$

for which ρ is the water density (1000 kg/m³), g is the gravitational acceleration (9.81 m/s²), Δz is the fault equivalent porous medium thickness (1 m) and μ is the water viscosity at 8°C (1.4×10-3 kg/m*s). The result is an apparent hydraulic conductivity of 2.4×10-4 m/s.

3.4 Sensitivity analysis

In order to target the best grouting scenario to reduce water inflow into the stope, a sensitivity analysis of variable pre-grouting approaches (cases) is performed on each model. For each case, a series of 10 simulations with varying hydraulic conductivity of the targeted grouted area is executed. For example, if the grouted area is the fault itself, the hydraulic conductivity will be reduced gradually from 2.4×10^{-4} m/s to 2.4×10^{-6} m/s. If the grouted area is the host rock, the hydraulic conductivity of the injected area will be reduced from 1.0×10^{-8} m/s to 1.0×10^{-10} m/s. The parameters investigated are mainly the hydraulic conductivity of the grouted area and its dimension. All simulated cases for Models A1 and A2 are presented in Figure 5 below and in Figure 6 for Model B.

For Models A1 and A2, case 1 corresponds to an injection of cement targeting a 1 m thick area between the stope and the fault.

Case 2 is similar, but the injection height covers the entire 2 m thick zone between the stope and the fault. For case 3, case 1 is reproduced with a larger span of 2 m on both sides of the injection zone. Case 4 is presented as the injection of cement directly into the fault, as wide as the stope's lateral extents. Case 5 combines grouting of the fault itself and of a 1 m thick area between the stope and the fault.

For case 1 of Model B, the design aims to seal the fault over a width of 3 m at its intersection with the stope, on both sides. Case 2 is the same operation for a wider span of 6 m on each side. Case 3 is designed to seal a part (11 m long) of the lateral limits of the stope. The height of 11 m is set upon the assumption that 5 m above and beneath the fault are sealed over a 3 m wide range. Case 4 expands the height to the lateral boundary extents. Grout penetration is considered optimal for the purpose of this paper. Also, Hernqvist & al. (2009) have shown that for larger fracture apertures, it is reasonable to assume that sealing with cement grouting can be achieved.

The code outputs used for the analysis are the velocities on every stope boundary element. The velocities are multiplied by the porosity and the element length on which they apply (1 m or 0.25 m) and summed up to obtain the total flux (q) towards the stope (per meter length of the stope), which are the results that are used as the basic comparison tool for the investigated scenarios.

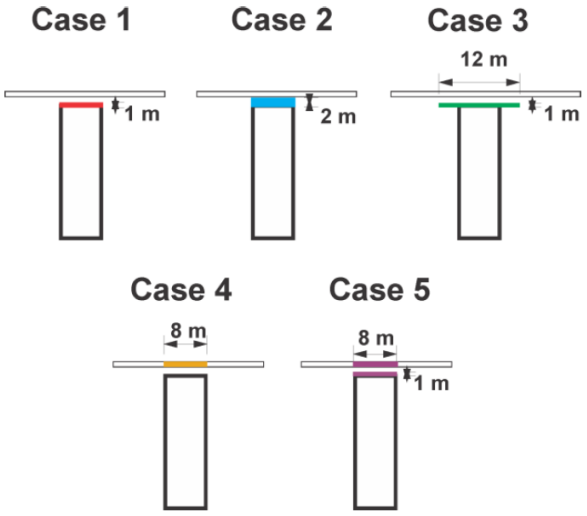

Figure 5. Simulated cases for Models A1 and A2

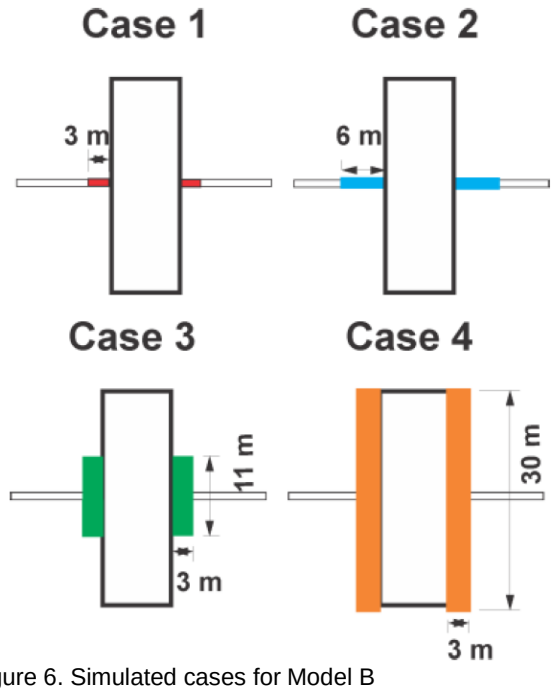

Figure 6. Simulated cases for Model B

4 RESULTS

The results of the sensitivity analysis are shown in terms of total flux q (m2/s) directed into the stope (volumetric flux m^3/s per m stope length). The flux reduction is always compared to the base case scenario, before the pregrouting simulation. The results are presented in two sections, to distinguish Models A1 and A2 results from Model B results.

4.1 Models A1 and A2

The simulated groundwater flow field before pre-grouting is shown as hydraulic heads and velocity vectors in Figure 7 for Model A1.

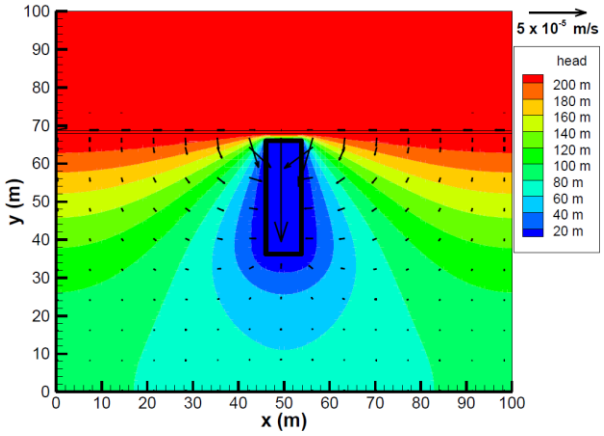

Figure 7. Simulated hydraulic heads and velocity vectors for Model A1 base case scenario

Before pre-grouting, the hydraulic heads above the stope are high and the velocity vectors are directed toward the stope, mainly towards its upper limit. The flux entering the stope for the base case scenario is 2.03×10^{-5} m²/s. Results for each case are compared to this value, as illustrated in the graph of influx as a function of the hydraulic conductivity of the rock mass presented in Figure 8.

From this figure, the most efficient pre-grouting method is the case 3 approach, with a flux of 8.70×10^{-6} m²/s at a *K* of 10^{-10} m/s, which represents a 57% reduction of the base case scenario value. Nevertheless, for higher hydraulic conductivities, between 9.0×10^{-9} m/s and 4.0×10^{-9} m/s, the flux is lower with the case 2 approach.

Cases 4 and 5 sensitivity analysis results are presented in Figure 9 showing the flux into the stope versus the fault hydraulic conductivity.

As seen in Figure 9, case 4 does not provide any reduction in fluxes for a decreasing fault hydraulic conductivity compared to the base case scenario. For a two-order of magnitude reduction of the hydraulic conductivity, the flux in case 5 decreases to 1.13×10-5 m²/s, which represents a 44% reduction of the base case scenario.

. Investigating the impact of adding a regional flux of 1×10-8 m/s from left to right into Model A, Model A2 results do not differ significantly from Model A1. Before pregrouting, the flux entering the stope is 2.01×10-5 m²/s, compared to 2.03×10-5 m²/s for the Model A1 without regional flow. All runs for each of the 5 cases of Model A1 were also conducted for Model A2 and results were compared. The greatest relative difference between these two scenarios is in the order of 3%, for case 3. For this particular case, a graph of the flux entering the stope with regional flow (A2) compared to the fluxes without regional flow is shown in Figure 10.

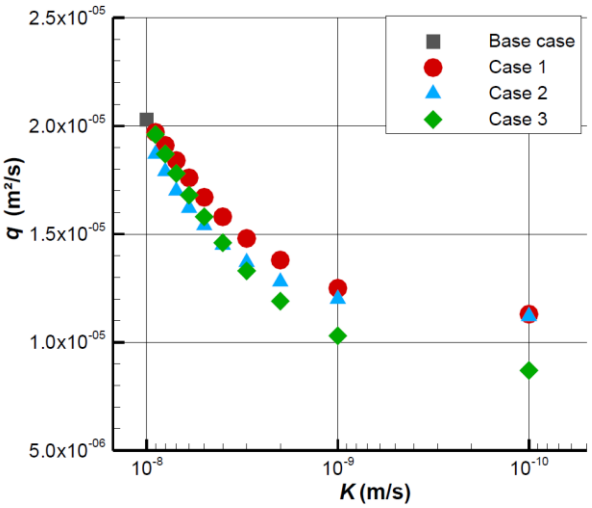

Figure 8. Flux into the stope vs. hydraulic conductivity of the rock mass for Model A1, cases 1 to 3. Total volumetric fluxes into the stope (m_3/s) can be obtained by multiplying by the stope length.

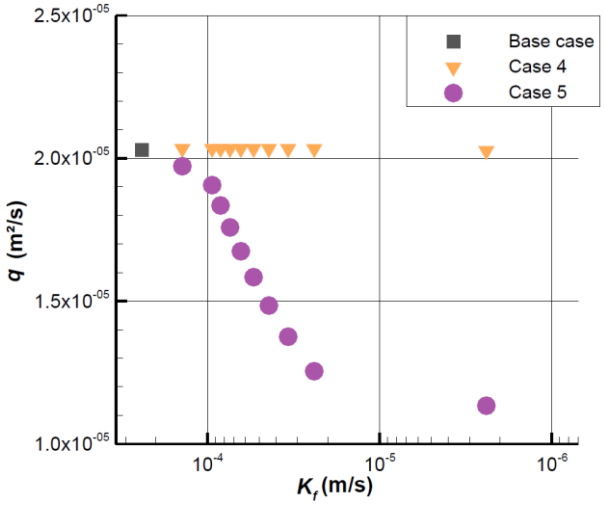

Figure 9. Flux into the stope vs. the fault hydraulic conductivity for Model A1, cases 4 & 5

Small differences are visible between the results of Model A1 and Model A2 illustrated on this graph. However the differences are very low and do not change the global results of the analysis for which case 3 is the best approach. This arguably supports the choice of not conducting an analysis with a regional flow for model B.

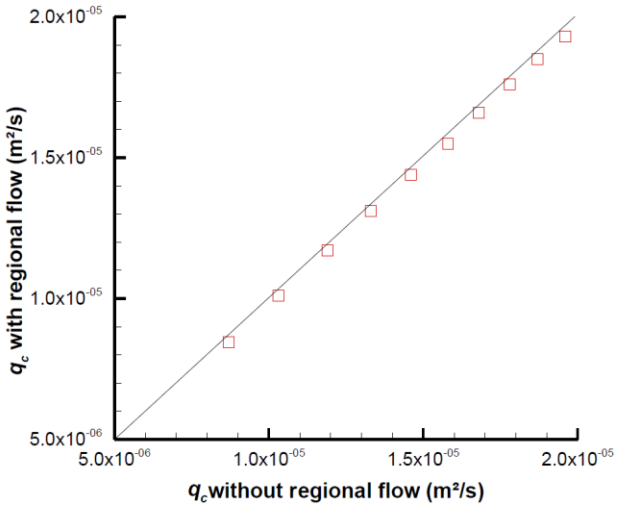

Figure 10. Comparison of the flux for Models A2 and A1

4.2 Model B results

The simulated hydraulic heads and velocity vectors before pre-grouting are shown in Figure 11 for Model B.

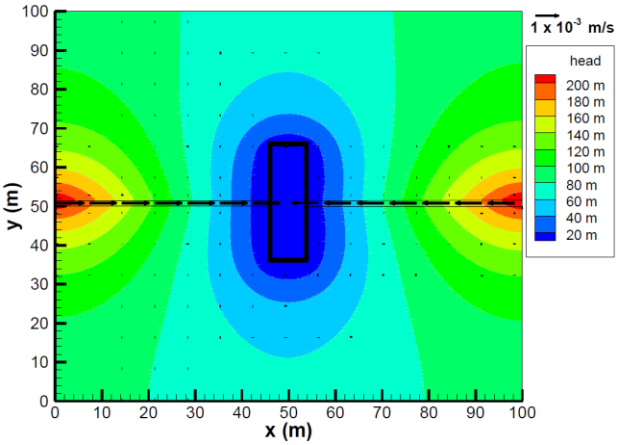

Figure 11. Simulated hydraulic heads and velocity vectors for Model B base case scenario

Before pre-grouting, the hydraulic head is higher where the fault intersects the model boundaries, at the location of the fixed head conditions. Also, the highest velocity vectors are located within the fault and directed toward the stope. The flux entering the stope for the Model B base case (ungrouted) is 1.44×10^{-5} m²/s.

All results for each case are compared to this value, as shown in Figure 12. The graph shows the reduction influx entering the stope as the fault hydraulic conductivity is decreased for Model B, cases 1 to 4.

The best performance approach is identified as case 2 (Figure 12), offering the lowest flux entering the stope for all hydraulic conductivities. The final flux, for a fault hydraulic conductivity two orders of magnitude less, is 1.36×10^{-4} m²/s, representing a 93% reduction of the base case flux.

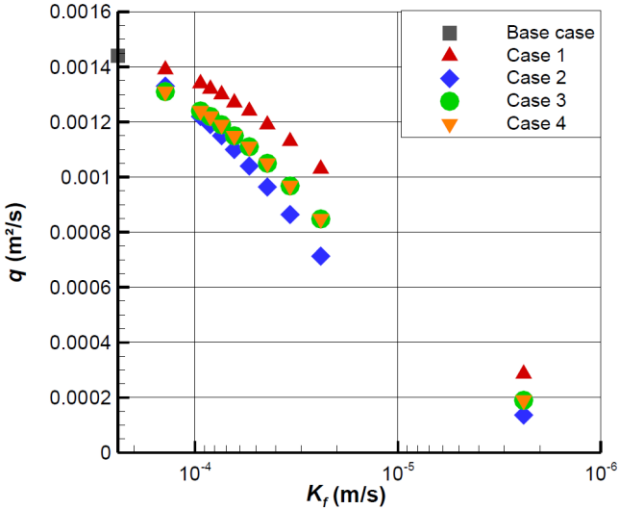

Figure 12. Flux into the stope vs. the fault hdraulic conductivity for Model B, cases 1 to 4

5 DISCUSSION

The sensitivity analysis results have shown the best approach for the two conceptual models at the Éléonore mine level 230. For a conceptual model of a fault located above the stope, the best approach is to inject cement into the area located between the stope and the fault, for an extent larger than the stope. The inflow reduction for this approach is 57% compared to the flux entering an ungrouted medium in Model A1. For a case with a fault intersecting the stope, the best approach consists of sealing the fault to the largest possible extent (6 meters on both side of the stope in this analysis), which would reduce the hydraulic conductivity of the grouted area by two orders of magnitude. This approach offers a 93% reduction of the influx compared to the ungrouted base case. Furthermore, it has been shown that since the maximum difference is only 3% between Model A1 and Model A2 results, the impact of regional flow can be neglected in the analysis.

As a comparison, Kvartsberg & Fransson (2013) showed that for a reduction of transmissivity by two orders of magnitude due to grouting, the inflow into a drift was reduced by 91%. This flux is much higher than the results obtained for Model A1 (57%) but is comparable to the results of Model B (93%).

Limitations of the model include its simplification to a 2D homogeneous model, which neglects the impact of transverse flow and may lead to an overestimation of the flux entering the stope, in all ungrouted and grouted cases.

Also, assuming a homogeneous rock mass may underestimate the inflow, since other structures may be present in the rock mass which may conduct water to the stope. The constant aperture of the fault itself is also a concern because a reduced aperture would lead to a reduced hydraulic conductivity and a lower flux entering the stope.

Finally, the cement properties are not considered in the analysis and may have an impact on the performance of the reduction of the hydraulic conductivity of the grouted zone. Characteristics such as grout penetration, if

overestimated, would lead to a lower flux reduction once the targeted area is considered grouted. Grouting mix proportions and injection pressures are both properties that have also proven to impact pre-grouting performance (Funehag & Fransson, 2006; Hernqvist & al., 2009).

6 CONCLUSION

This study aimed at contributing to optimize the pre-grouting methodology for mining stopes at Goldcorp's Éléonore mine, in a zone where water inflows were linked to the major faults. A sensitivity analysis of pre-grouting approaches regarding 2 fault locations was conducted with a 2D groundwater flow numerical model.

The results showed that for a fault located above the stope, it is recommended to grout the area between the stope and the fault, for a span larger than the stope lateral limits. This approach offered a 57% reduction of the flux entering the stope. Also, it has been observed that regional flow has a negligible impact on the flux entering the stope.

For a fault intersecting the stope, it is suggested to grout the fault directly, for a length of at least 6 m on both sides of the stope, in the investigated case of an 8 m wide stope. This approach offered a 93% reduction of the inflow into the stope.

As recommendations for future work, the two suggested designs may be applied to similar occurring cases at the underground mine, to verify the performance of the mitigation approach. Also, an investigation into the impact of the fault location above the stope with respect to the flux reduction results would set the limits of the most promising approach. Finally, an investigation into the influence of the grouting approach on inflow reduction should be performed considering penetration rate and efficiency.

7 REFERENCES

Coli, M. & Pinzani, A. (2014). Tunneling and hydrogeological issues: A short review of the current state of the art. *Rock Mechanics and Rock Engineering*, 47(3): 839-851. doi: 10.1007/s00603-012-0319-x

Domingue, C. (2017). Modélisation 3D de l'écoulement de l'eau souterraine et évaluation de l'efficacité de différentes méthodes de cimentation pour la réduction d'infiltrations d'eau à la mine Éléonore, Master's Thesis, Laval University, Quebec City, Quebec, Canada, 101 p.

Fontaine, A., Dubé, B., Malo, M., McNicoll, V. & Brisson, T. (2015a). Géologie et caractéristiques structurales du gisement aurifère Roberto, propriété Éléonore, Province du Supérieur, Baie-James, Québec, Canada. *Abstracts of oral presentations and posters : Québec Mines 2014*, Ministère de l'Énergie des Ressources Naturellles du Québec, Québec, DV 2015-04, 68 pp.

Funehag, J. & Fransson, A. (2006). Sealing narrow fractures with a Newtonian fluid: Model prediction for grouting verified by field study, *Tunnelling and Underground Space Technology*, 21(5): 492–498, doi:10.1016/j.tust.2005.08.010

Goldcorp Inc. (2014). Eleonore Structural Model, Interoffice memorandum. Eleonore Mine, Goldcorp Inc., Quebec, Canada.

Goldcorp Inc. (2017). Internal note. Eleonore Mine, Goldcorp Inc., Quebec, Canada.

Golder Associates Ltd. (2009). Hydrogeological study of the proposed underground mine (original 2007 design - 3500 t/day), Eleonore Project. Internal report.

Hernqvist, L., Fransson, Å., Gustafson, G., Emmelin, A., Eriksson, M., & Stille, H. (2009). Analyses of the grouting results for a section of the APSE tunnel at Äspö Hard Rock Laboratory. *International Journal of Rock Mechanics and Mining Sciences*, 46(3): 439-449. doi: 10.1016/j.ijrmms.2008.02.003

Holmøy, K. H. & Nilsen, B. (2014). Significance of geological parameters for predicting water inflow in hard rock tunnels. *Rock Mechanics and Rock Engineering*, 47(3): 853-868. doi: 10.1007/s00603-013-0384-9

Kvartsberg, S. and Å. Fransson (2013). Hydrogeological characterisation and stochastic modelling of a hydraulically conductive fracture system affected by grouting: A case study of horizontal circular drifts. *Tunnelling and Underground Space Technology*, 38: 38-49. doi:10.1016/j.tust.2013.05.007

Manda, A. K., Mabee, S. B., Boutt, D. F., Cooke, M. L. (2013). A method of estimating bulk potential permeability in fractured-rock aquifers using field-derived fracture data and type curves. *Hydrogeology Jour.*, 21: 357-369. doi: 10.1007/s.10040-012-0919-2.

Molson, J. & Frind, E. (2017). FLONET/TR2, User Guide Version 5.0; A Two-Dimensional Simulator for Groundwater Flownets, Contaminant Transport and Residence Time. Université Laval & University of Waterloo, 57 pp.

Park, Y.-J., Sudicky, A. & McLaren R.G. (2004). Analysis of hydraulic and tracer response tests within moderately fractured rock based on transition probability geostatistical approach. *Water Resources Research*, 40: 1-14, W12404. doi:10.1029/2004WR003188

Ravenelle, J.-F., Dubé, B., Malo, M., McNicoll, V., Nadeau, L. & Simoneau, J. (2010). Insights on the geology of the world-class Roberto gold deposit, Éléonore property, James Bay area, Quebec. *Geological Survey of Canada*, Current Research 2010-1, 26 p.